

## A model experiment of damage detection for offshore jacket platforms based on partial measurement

Shi Xiang<sup>†</sup>, Li Hua-jun<sup>‡</sup>, Yang Yong-chun<sup>††</sup> and Gong Chen<sup>‡‡</sup>

Engineering College, Ocean University of China, Qingdao, 266100, China

(Received August 28, 2006, Accepted December 27, 2007)

**Abstract.** Noting that damage occurrence of offshore jacket platforms is concentrated in two structural regions that are in the vicinity of still water surface and close to the seabed, a damage detection method by using only partial measurement of vibration in a suspect region was presented in this paper, which can not only locate damaged members but also evaluate damage severities. Then employing an experiment platform model under white-noise ground excitation by shaking table and using modal parameters of the first three modes identified by a scalar-type ARMA method on undamaged and damaged structures, the feasibility of the damage detection method was discussed. Modal parameters from eigenvalue analysis on the structural FEM model were also used to help the discussions. It is demonstrated that the damage detection algorithm is feasible on damage location and severity evaluation for broken slanted braces and it is robust against the errors of baseline FEM model to real structure when the principal errors is formed by difference of modal frequencies. It is also found that Z-value changes of modal shapes also play a role in the precise detection of damage.

**Keywords:** damage detection; offshore jacket platform; model experiment; partial measurement; shaking table.

---

### 1. Introduction

The field of health monitoring and damage detection has a great potential for applications in offshore structures (Roesset and Yao 1998). In general, offshore platforms in deep water have to face harsh marine environments, withstanding cyclic waves, severe storms, seaquakes and sea-water corrosion. The occurrence of damage in an offshore structure is inevitable during its lifetime. Therefore, aging structures must be inspected at regular intervals in order to detect the initiation and growth of damages that may lead to catastrophic failure. Currently, divers or Remote Operated Vehicles (ROV) are employed for the purpose of visual inspection and damage detection by local techniques such as X-ray and ultrasonic methods. However, the process of inspection and local detection for offshore structures, especially in deep water, is much more difficult than for land

---

<sup>†</sup> Associate Professor, Corresponding author, E-mail: shixiang@ouc.edu.cn

<sup>‡</sup> Professor, E-mail: huajun@ouc.edu.cn

<sup>††</sup> Professor, E-mail: yycyw@ouc.edu.cn

<sup>‡‡</sup> Master Student, E-mail: jett\_fun555@sina.com

\*The project was financially supported by the Cultivation Fund of the Key Scientific and Technical Innovation Project (Grant No. 704031) and the Scientific Research Foundation for the Returned Overseas Chinese Scholars, Ministry of Education of China.

structures. The poor visibility and the concealment of damage by marine growth limit the effectiveness of process technically. In addition, the use of divers and/or ROV is very costly. It is impractical to inspect the huge structural system completely at a time. Generally an optimal IRM (Inspection, Repair and Maintenance) plan is established by compromising between the reliability and the cost (Della Greca 1997). So it is strongly requested to develop a global technique capable of assessing the health of offshore structures in an automated fashion, providing advance warning of structural damages and minimizing maintenance costs (Nichols 2003). Also the approximate damage locations are requested to provide prior to implementing the underwater inspection or local detection.

In response to these requests, a substantial amount of activities related to the global health monitoring and damage detection for offshore platforms have been carried out during the past decades. Among these activities, vibration-based approaches (Kondo and Hamamoto 1994, Kim and Stubbs 1995, Brincker *et al.* 1995, Doebling *et al.* 1998, Ruotolo *et al.* 2000, Mangal *et al.* 2001, Sanderson *et al.* 2002, Yang *et al.* 2003, Shi *et al.* 2005) have been widely employed, which detect the changes of structural modal properties. The basic idea behind this technology is that the modal parameters (natural frequencies, mode shapes, and modal damping) are functions of physical properties of the structure (mass, stiffness, and damping). Therefore, changes in the physical properties will cause detectable changes in the modal properties (Doebling *et al.* 1998).

The majority of offshore platforms are jacket-type, steel tubular, space frames. Generally this type of offshore platform consists of hundreds of members and joints. From the experience of underwater inspections (Della Greca 1997, Stacey and Sharp 1997), it can be noted that there are two regions of structure where damage incidents occur most frequently. One such region is in the vicinity of still water surface where the wave force is most violent. It is reported that wave slamming by storms, seawater corrosion and ship collision usually take place in this region. The other region is close to the seabed where the bending moment on the platform legs exerted by environmental loads is largest and the water pressure is highest for platforms in deep water. Recognizing the fact that the damage occurrence is concentrated in these two regions and that it is hardly possible to install sensors at every joint of the huge structural system, Shi *et al.* (2005) proposed a damage location method based on partial measurement of vibration (i.e., detecting damages in a suspect region) and checked the feasibility of it by employing a numerical model of an offshore jacket platform under white-noise ground excitation.

In this paper, applying the algorithm of mode shape expanding (Shi *et al.* 2005) to an improved damage detection algorithm (Kim and Stubbs 2002), a damage detection method for offshore jacket platforms, which can not only locate damaged members but also evaluate damage severity by using only partial measurement of vibration and few lower modes, was presented at first. Then employing an experiment platform model under white-noise ground excitation by shaking table and using modal parameters of undamaged and damaged structures identified by a scalar-type ARMA method (Kanazawa and Hirata 2000), the feasibility of the damage detection method was discussed. Modal parameters from FEM analysis were also used to help the discussions.

## 2. Damage detection algorithm

### 2.1 An existing algorithm for damage detection using whole mode shapes

For a linear, undamaged, skeletal structure with  $ne$  elements and  $n$  nodes, the  $i$ th modal stiffness

of the arbitrary structure is given by

$$S_i = \{\Phi_i\}^T [K] \{\Phi_i\} \quad (1)$$

where  $\{\Phi_i\}$  is the  $i$ th whole modal vector and  $[K]$  is the system stiffness matrix. The contribution of the  $j$ th member to the  $i$ th modal stiffness  $S_{ij}$  is given by

$$S_{ij} = \{\Phi_i\}^T [K_j] \{\Phi_i\} \quad (2)$$

where  $[K_j]$  is the contribution of the  $j$ th member to the system stiffness matrix.

Let the corresponding modal parameters in Eqs. (1) to (2) associated with a subsequently damaged structure be characterized by asterisks. Then for the damaged structure, it has

$$S_i^* = \{\Phi_i^*\}^T [K^*] \{\Phi_i^*\} \quad (3)$$

$$S_{ij}^* = \{\Phi_i^*\}^T [K_j^*] \{\Phi_i^*\} \quad (4)$$

The quantities  $[K_j]$  and  $[K_j^*]$  in Eqs. (2) and (4) may be written in a standard formation by FEM as follows

$$[K_j] = E_j [K_{j0}]; \quad [K_j^*] = E_j^* [K_{j0}] \quad (5)$$

where the scalars  $E_j$  and  $E_j^*$  are parameters representing material stiffness properties of undamaged and damaged  $j$ th member of the structure, respectively (for simplicity, they can be regarded as Young's modulus), and the matrix  $[K_{j0}]$  involves only geometric quantities. The ratio  $E_j/E_j^*$  can be regarded as a damage-location indicator for the  $j$ th member.

Let  $dS_{ij}$  represent the fractional change in  $S_{ij}$ ,  $\lambda_i$  and  $\lambda_i^*$  represent the  $i$ th eigenvalues of pre- and post-damage MDOF structural system respectively. Assuming the structure is damaged in  $nd$  locations, the fractional changes in modal stiffness can be approximately related to the fractional changes in modal properties (Kim and Stubbs 2002) in the form

$$\frac{dS_{ij}}{S_i} \cong g_i(\lambda, \Phi) = \left( \frac{d\lambda_i}{\lambda_i} + \frac{dM_i}{M_i} \left( 1 + \frac{d\lambda_i}{\lambda_i} \right) \right) / nd \quad (6)$$

in which  $g_i(\lambda, \Phi)$  is the dimensionless factor representing the systematic change in modal parameters of the  $i$ th mode due to the damage.  $d\lambda_i = \lambda_i - \lambda_i^*$  (usually  $\lambda_i > \lambda_i^*$ ).  $dM_i$  is the change of the  $i$ th modal mass  $M_i$  in the system. Herein  $dM_i$  is set to be zero because its weight is small on calculation and it is difficult to be obtained when the modal mass  $M_i$  is not set to be unity.

Then a damage index for  $i$ th mode and  $j$ th location is given by

$$\beta_{ji} = \frac{E_j}{E_j^*} = \frac{\gamma_{ij}^*}{\gamma_i g_i(\lambda, \Phi) + \gamma_{ij}} = \frac{Num}{Den} \quad (7)$$

in which

$$\gamma_{ij}^* = \{\Phi_i^*\}^T [K_{j0}] \{\Phi_i^*\}, \quad \gamma_i = \sum_{k=1}^{ne} \{\Phi_i\}^T [K_{k0}] \{\Phi_i\}, \quad \gamma_{ij} = \{\Phi_i\}^T [K_{j0}] \{\Phi_i\} \quad (8)$$

For  $nm$  vibration modes, a damage index  $\beta_j$  for the  $j$ th location is obtained by

$$\beta_j = \sum_{i=1}^{nm} Num / \sum_{i=1}^{nm} Den \quad (9)$$

Once damage is localized at the  $j$ th member, its severity can be estimated as

$$\alpha_j = dE_j/E_j = 1/\beta_j - 1, \quad \alpha_j \geq -1 \quad (10)$$

where damage severity is indicated as the reduction in stiffness in the  $j$ th member if  $\alpha_j < 0$ .

## 2.2 Improved algorithm using partial mode shapes

In the damage detection algorithm discussed above, the mode shapes at all nodes of the structure are requested as shown by Eq. (8). However, in a real situation, it is hardly possible to install sensors at every joint of such a huge structural system as an offshore platform. Therefore it is desirable to use only partial measurement at nodes in a suspect region to realize the calculation of damage detection. In the following, such an algorithm (Shi *et al.* 2005), which can expand partial modal shape to whole modal shape by employing the stiffness and mass matrices from FEM model, is introduced by assuming that the damaged members are located only in the detecting region (i.e., they are among the members connected by the measured nodes).

Assume that the dynamic equation of motion for an undamaged skeletal structure can be written in the form

$$[M]\{\ddot{U}\} + [C]\{\dot{U}\} + [K]\{U\} = \{F\} \quad (11)$$

where  $[M]$ ,  $[C]$  and  $[K]$  represent the mass, damping and stiffness matrices of the structural system respectively ( $[M]$  is assumed to have the form of lumped mass approximation), and  $\{\ddot{U}\}$ ,  $\{\dot{U}\}$  and  $\{U\}$  denote the vectors of structural accelerations, velocities and displacements respectively. Noting that actually only translational accelerations can be measured by sensors, it is treated at this stage to apply the static condensation technique to condense the  $[K]$ ,  $[M]$  and  $[C]$  matrices with only three translational DOFs for every node item.

Let the  $[K]$  and  $[M]$  matrices be decomposed into measured and unmeasured node items as follows

$$[K] = \begin{bmatrix} K_{uu} & K_{um} \\ K_{um}^T & K_{mm} \end{bmatrix}, \quad [M] = \begin{bmatrix} M_{uu} & 0 \\ 0 & M_{mm} \end{bmatrix} \quad (12)$$

in which subscripts  $m$  and  $u$  represent measured and unmeasured node items, respectively. It is suggested that the measured nodes had better be selected to be consecutive.

Then the equation of motion for free vibration analysis can be written in the form

$$\left( \begin{bmatrix} K_{uu} & K_{um} \\ K_{um}^T & K_{mm} \end{bmatrix} - \omega_i^2 \begin{bmatrix} M_{uu} & 0 \\ 0 & M_{mm} \end{bmatrix} \right) \begin{Bmatrix} \Phi_{iu} \\ \Phi_{im} \end{Bmatrix} = \begin{Bmatrix} 0 \\ 0 \end{Bmatrix} \quad (13)$$

where  $\omega_i$  is the natural circular frequency of  $i$ th mode, and  $\Phi_{iu}$  and  $\Phi_{im}$  are the  $i$ th mode shapes at unmeasured and measured nodes, respectively. Decomposing Eq. (13) and by substitution, the  $i$ th

mode shape of unmeasured nodes,  $\Phi_{iu}$ , can be obtained from the partial mode shape associated with measured nodes,  $\Phi_{im}$ , by

$$\Phi_{iu} = -(K_{uu} - \omega_i^2 M_{uu})^{-1} K_{um} \Phi_{im} \quad (14)$$

Thus the  $i$ th mode shape at all nodes is expressed as

$$\{\Phi_i\} = \begin{Bmatrix} \Phi_{iu} \\ \Phi_{im} \end{Bmatrix} = \begin{Bmatrix} R \\ I \end{Bmatrix} \{\Phi_{im}\} \quad (15)$$

where

$$R = -(K_{uu} - \omega_i^2 M_{uu})^{-1} K_{um} \quad (16)$$

Also let the corresponding items in Eqs. (15) and (16) associated with a subsequently damaged structure be characterized by asterisks. Then the following relations can be obtained

$$\{\Phi_i^*\} = \begin{Bmatrix} \Phi_{iu}^* \\ \Phi_{im}^* \end{Bmatrix} = \begin{Bmatrix} R^* \\ I \end{Bmatrix} \{\Phi_{im}^*\} \quad (17)$$

where

$$R^* = -(K_{uu}^* - \omega_i^{*2} M_{uu}^*)^{-1} K_{um}^* \quad (18)$$

Assuming that the damage members are among the members connected by the measured nodes, it can be approved that

$$K_{uu}^* = K_{uu}, \quad K_{um}^* = K_{um}, \quad M_{uu}^* = M_{uu} \quad (19)$$

Then Eq. (18) can be rewritten in the form

$$R^* = -(K_{uu} - \omega_i^{*2} M_{uu})^{-1} K_{um} \quad (20)$$

Using Eqs. (15), (16), (17) and (20), the mode shapes at all nodes in pre- and post-damaged structures can be obtained from the partial mode shapes at measured nodes and the associated natural frequencies. Thus, employing Eqs. (9) and (10), the damaged member can be detected using only partial measurement of vibration. Then for real situation, the modal parameters only needed to identify are  $\Phi_{im}$ ,  $\Phi_{im}^*$ ,  $\omega_i$  and  $\omega_i^*$ . It is important to note that the improvement does not alter the algorithm itself, but is just a supplement to it by mode shape expanding.

The indicator of damage location  $\beta_j$  is normalized to provide more robust statistical criteria for damage location. The normalized damage index for the  $j$ th member,  $Z_j$ , is given by

$$Z_j = \frac{\beta_j - \bar{\beta}}{\sigma_\beta} \quad (21)$$

where the terms  $\bar{\beta}$  and  $\sigma_\beta$  represent the mean and the standard deviation of the collection of  $\beta_j$  values (for the members located in the detecting region), respectively.

The damage pattern is classified via a statistical-pattern-recognition technique using hypothesis

testing. Then the decision rule for damage location is selected as follows (Fukunaga 1990):

The structure is not damaged at the  $j$ th location when  $Z_j < Z_c$ ;

The structure is damaged at the  $j$ th location when  $Z_j \geq Z_c$ ;

in which  $Z_c$  is a number that reflects the level of significance of the test (e.g., if  $Z_c = 2$ , then the confidence level is 97.7%). It should be mentioned that the following figures in Section 3 for damage location will use index  $Z_j$ .

In final, the damage-detection algorithm can be summarized with the following characteristics:

- (1) only a few modes (i.e., less than or equal to two modes) are available,
- (2) only partial measurement is available (i.e., damages in suspect structural region can be detected),
- (3) three translational DOFs are measured by sensors at a node.

### 3. Experiment analysis

#### 3.1 General description of the experiment

A four-layered, three-dimensional steel frame was fabricated to represent a typical offshore jacket platform, as shown in Fig. 1. Its jacket template is 2.4 m high, 600 mm  $\times$  400 mm on the bottom and 375 mm  $\times$  250 mm on the top. The experimental model is constructed of steel tubes, using 14 mm  $\times$  2 mm (outer diameter  $\times$  thickness) section as 4 legs and 10 mm  $\times$  2 mm section as all braces, and a steel plate at the top with a thickness of 20 mm to simulate the upside structure.

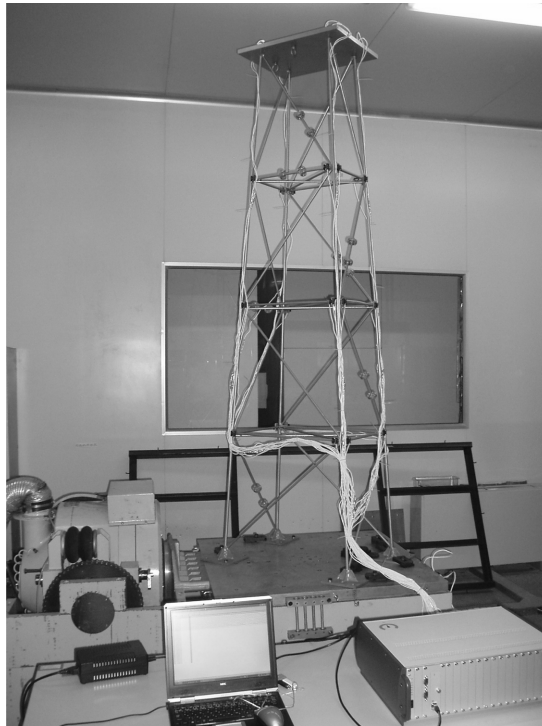


Fig. 1 The experiment model and instruments

Several exchange parts connecting brace were made in the model to simulate the member damage. As shown in Fig. 2, removing all the bolts in two flanges and taking the exchange part out, the member is damaged completely. Re-installing the exchange part, the damaged member recovers. In addition, an alternative exchange part with 6 mm × 1 mm (outer diameter × thickness) section, which can instead of the intact exchange part with 10 mm × 2 mm section, is prepared for simulating the cases of partly damaged member.

The instruments consisted of an electro-dynamic vibrator (DY-1000-8, Suzhou Testing Instrument General Factory, China) for exerting ground acceleration, 33 capacitive accelerometers (Model 2220-005, Silicon Designs Inc., U.S.A) for response measurement and a measurement system (PL16-DCB8, Integrated Measurement & Control Cooperation, Germany) for data acquisition. 32 accelerometers were installed on each intersection point between brace and leg in both X and Y directions, and the last one was installed on the shaking table to measure ground acceleration. The experimental model was rigidly fixed on the shaking table where its X-axis was 45 degrees relative

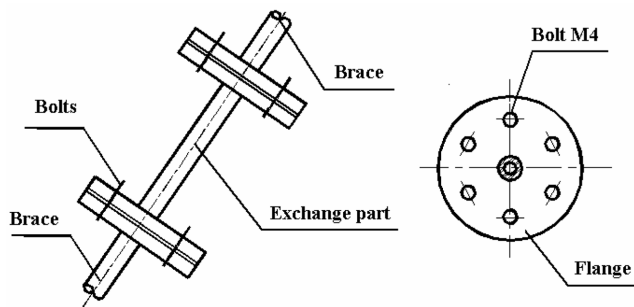


Fig. 2 Exchange part to simulate member damage

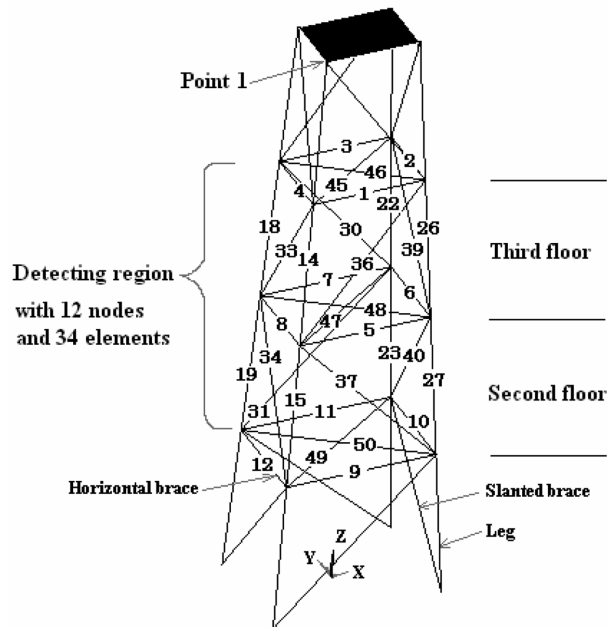


Fig. 3 The FEM model and damage detecting region

to the vibrating direction so as to excite the structural modes in all directions. The input acceleration to shaking table was set to be a white noise with RMS of  $0.98 \text{ m/s}^2$  ranging from 2 Hz to 200 Hz. The sampling frequency for each measurement channel was set to be 500 Hz.

The FEM model of the experimental model was subsequently established, as shown in Fig. 3. It has totally 20 nodes constructing 50 pipe elements, 1 shell element and 4 lumped-mass elements on the top floor. The model was assumed to be fixed at four nodes on the ground (shaking table). The material of all structural members is steel with mass density of  $7,800 \text{ kg/m}^3$ , Young's modulus of 207 GPa (for undamaged state) and Poisson's ratio of 0.3. The structural region between the second and third floors was selected as the damage-detecting region. There are totally 12 nodes and 34 elements in this region. So actually measurement data from only 27 accelerometers between the second and third structural floors and on point 1 and shaking table, which represented the partial measurement, was used in this experiment. Positions of the 34 elements are also marked in Fig. 3. The member order of the 34 elements denoted in the figures of damage indices below is listed in Table 1.

Considering the fact that braces were usually damaged in jacket-type platforms, seven damage cases only for braces, inflicted in the damage detecting region, are investigated. As listed in Table 2,

Table 1 Element numbers in the detecting region

MO*	EN**	MO	EN	MO	EN	MO	EN
<u>1</u>	1	<u>10</u>	10	<u>19</u>	26	<u>28</u>	40
<u>2</u>	2	<u>11</u>	11	<u>20</u>	27	<u>29</u>	45
<u>3</u>	3	<u>12</u>	12	<u>21</u>	30	<u>30</u>	46
<u>4</u>	4	<u>13</u>	14	<u>22</u>	31	<u>31</u>	47
<u>5</u>	5	<u>14</u>	15	<u>23</u>	33	<u>32</u>	48
<u>6</u>	6	<u>15</u>	18	<u>24</u>	34	<u>33</u>	49
<u>7</u>	7	<u>16</u>	19	<u>25</u>	36	<u>34</u>	50
<u>8</u>	8	<u>17</u>	22	<u>26</u>	37		
<u>9</u>	9	<u>18</u>	23	<u>27</u>	39		

\*MO : Member Order, \*\*EN : Element Number.

Table 2 Damage cases inflicted in the detecting region

Case	Damaged member (Element number)	Located position	Damage severity* (%)
1	Slanted brace 30	Third floor / Back XZ plane	100
2	Slanted brace 39	Third floor / Right YZ plane	100
3	Slanted brace 40	Second floor / Right YZ plane	100
	Slanted brace 30	Third floor / Back XZ plane	100
4	Horizontal brace 1	Top of Third floor / Front XZ plane	100
5	Slanted brace 40	Second floor / Right YZ plane	100
	Horizontal brace 1	Top of Third floor / Front XZ plane	100
6	Slanted brace 30	Third floor / Back XZ plane	68.75
7	Slanted brace 39	Third floor / Right YZ plane	68.75

\*Damage severity: the reduction percentage in Young's modulus

the state of damaged braces for first five cases is severance namely the damage severity is 100%, among which three damage cases (Case 1, 2 and 4) are limited to the structure damaged only in a single location and two damage cases (Case 3 and 5) are for the structure damaged in two locations. The state of damaged braces for last two cases (Case 6 and 7), by employing the alternative exchange part, is partly damaged and the damage severity is approximately estimated as 0.6875 from the reduction ratio of section area.

### 3.2 Outline of modal identification

A scalar-type ARMA method (Kanazawa and Hirata 2000), which is a time-domain method only based on output data from ambient vibration measurement, was employed to identify the modal parameters of the experiment model. In performing the modal identification, point 1 on the top floor was selected as the reference point as shown in Fig. 3, and 12 nodes in the detecting region were selected as the measurement points. Including the channel to measure ground acceleration, actually only 27 channels of data that represented the partial measurement was used in this experiment. The total number of data for each channel was set to be 16384, consequently the data length was 32.768s. Accelerations relative to ground for all 13 points were calculated as the input data to modal identification. As an example, the relative accelerations at point 1 and the absolute acceleration on ground are shown in Fig. 4.

The natural frequencies and 12-point mode shapes (two dimensional) of the first three modes were identified for the undamaged case and each damaged case. The identified modal frequencies of the undamaged experiment model in contrast with the values evaluated from eigenvalue analysis on the FEM model are listed in Table 3. From the table, it can be noted that the first two modal

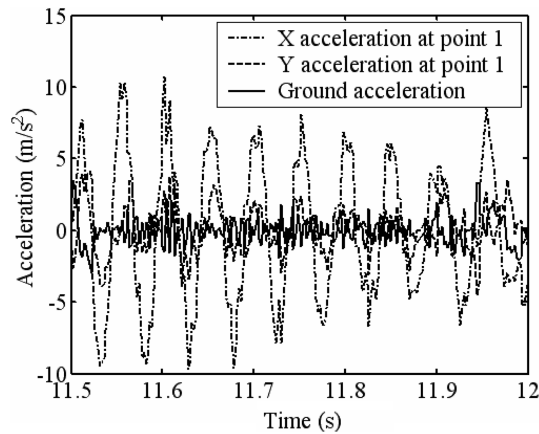


Fig. 4 Accelerations at point 1 and on ground

Table 3 Modal frequencies of FEM model and experiment model

Mode order	First	Second	Third
Mode direction	Y bending	X bending	Z torsion
FEM model (Hz)	17.39	25.19	41.35
Experiment model (Hz)	13.15	20.13	43.69

frequencies of the experimental model are smaller than those of the FEM model. This phenomenon is mainly attributed to the foundation stiffness of the shaking table that reduces the global stiffness of the whole experiment system but is not considered in the FEM model. It is found that the measured first two modal frequencies of the experiment model by impulse excitation are very close to those of the FEM model when it was once fixed on concrete ground directly. And the principal difference between the FEM model and the experiment structure is modal frequencies. When using the damage-detection algorithm aforementioned, Eqs. (8), (16) and (20) require the knowledge of the stiffness and mass matrices of undamaged structure, in fact which are from the baseline FEM model. Herein deviation existed between the FEM model and the experiment one obviously, model updating of the FEM model may be needed. But the following test results reveal that the damage indices defined by Eq. (9), of which the mechanism is to detect the changes of mode shapes, are very insensitive to the FEM model errors to the real structure when the principal errors is formed by difference of modal frequencies not by mode shapes.

### 3.3 Location of damages

Then the identified natural frequencies and 12-point mode shapes (two dimensional) of three modes for undamaged and damaged structures, associated with the stiffness and mass matrices from the FEM model without model updating, are used to analyze the five damage cases listed in Table 2. As mentioned before, when calculating the damage index  $\beta_j$ ,  $dM_i$  in Eq. (6) is set to be zero.

Figs. 5 to 7 show the results of damage location for first three damage cases where a single slanted brace was damaged for Case 1 and 2, and two slanted braces were damaged for Case 3. If the decision rule is set to be  $Z_c = 2$ , it can be observed that the four damage locations in three damage cases are correctly predicted. No false prediction is found in the three damage cases. And it is found that the stiffness and mass matrices from the FEM model without model updating are available for the calculation of damage location.

Herein the influence of  $Z$  value of nodal mode shape on damage location will be discussed. Theoretically three-dimensional modal shapes at a node are needed for the damage detection

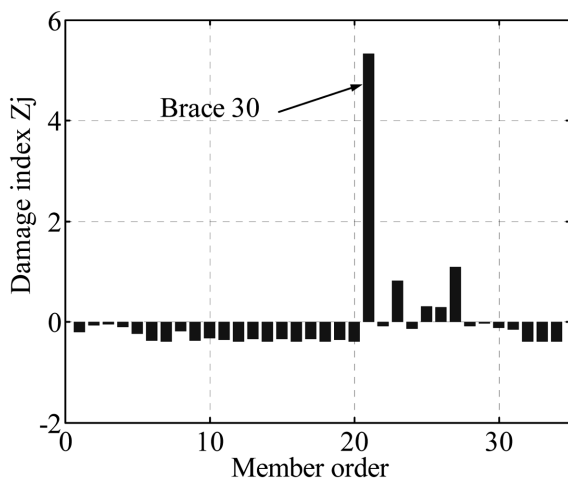


Fig. 5 Damage indices for Case 1

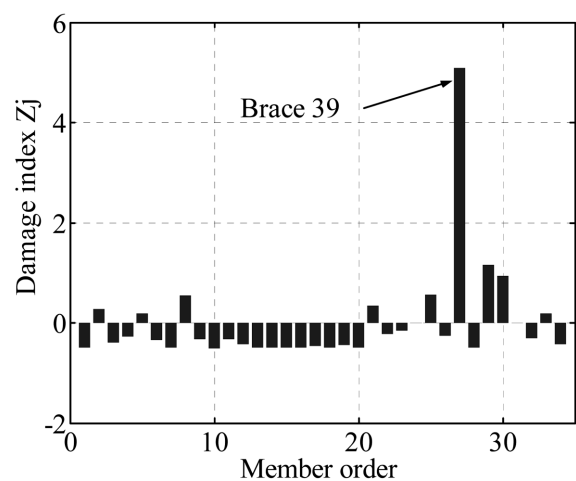


Fig. 6 Damage indices for Case 2

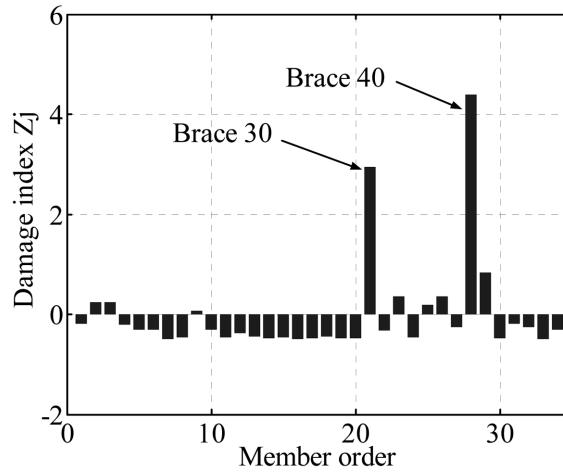


Fig. 7 Damage indices for Case 3

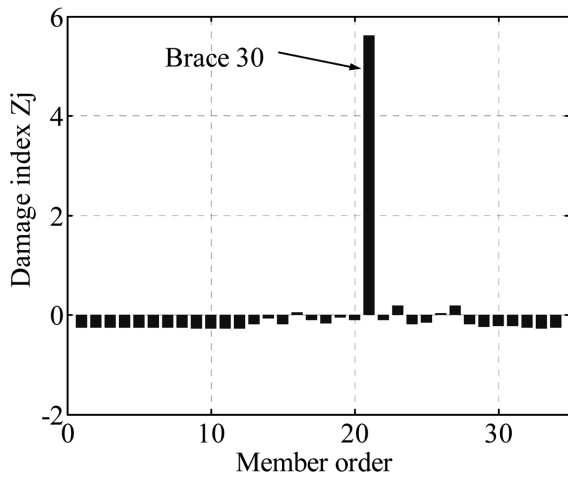


Fig. 8 Damage indices using three-dimensional modal shapes from FEM analysis for Case 1

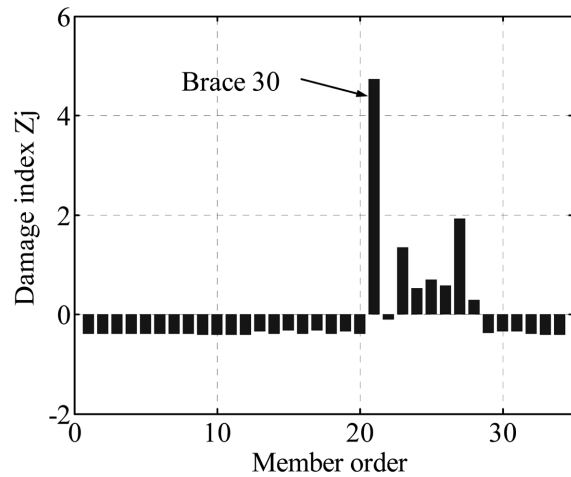


Fig. 9 Damage indices using two-dimensional modal shapes from FEM analysis for Case 1

algorithm as mentioned in Section 2. In the experiment, only two-dimensional accelerations at a point are measured so modal shapes without  $Z$  values at nodes have to be used in calculation. Despite that the  $Z$  value is relatively smaller than the  $X$  or  $Y$  values of modal shape for the first three modes, but it really play a role in the precise location of damage. As an example, Case 1 is employed to explain the influence of  $Z$  value of nodal mode shape on damage location. An FEM model corresponding to Case 1, in which the brace 30 is damaged completely, is created. Using the natural frequencies and 12-point mode shapes of the first three modes from eigenvalue analysis on the undamaged and damaged FEM models, the damage indices are calculated using three-dimensional and two-dimensional ( $Z$  values are set to be zero) modal shapes respectively. Fig. 8 shows the excellent result of damage location when using three-dimensional modal shapes. But Fig. 9 has some error predictions when using two-dimensional modal shapes. Comparing Fig. 4 with Fig. 9, it is found that the error predicted indices from experiment match the result from FEM analysis quit

well such as on member order 23 and 27. So it can be concluded that the Z-value changes of modal shapes influence the damage location in some extent but does not alter the eventual judgement for damaged brace.

Fig. 10 shows the result of damage location for Case 4 that a horizontal brace was damaged. It is noted that the damage location cannot be predicted and two false locations are found. It is analyzed that the inadequate prediction is mainly caused by the structural redundancy of horizontal brace. The complicated braces in the horizontal level including two diagonal braces lead that the horizontal brace is so redundant that its severance causes little change of the first three modes and the change is covered by other disturbance such as measurement noise. Further analysis are executed for Case 4, it is found that the horizontal brace can be located using one bending mode, as shown in Fig. 11. So it can be deduced that the little modal change caused by the damaged horizontal brace is covered by the identification errors on the other two modes.

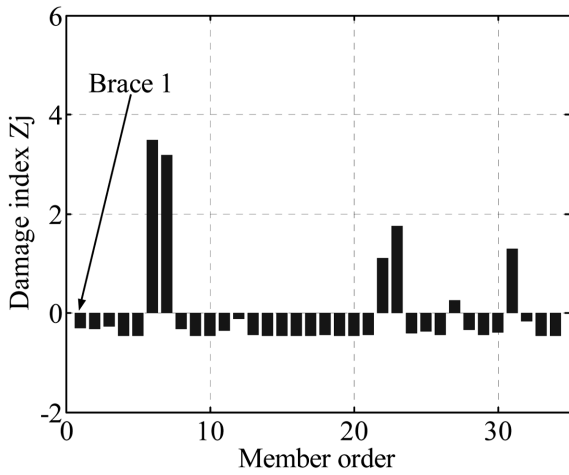


Fig. 10 Damage indices for Case 4

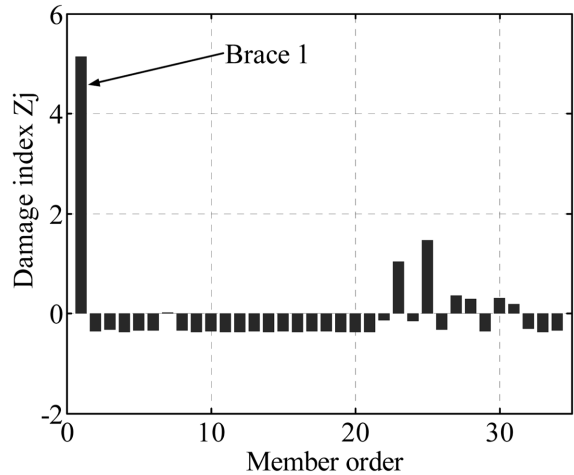


Fig. 11 Damage indices using one bending mode for Case 4

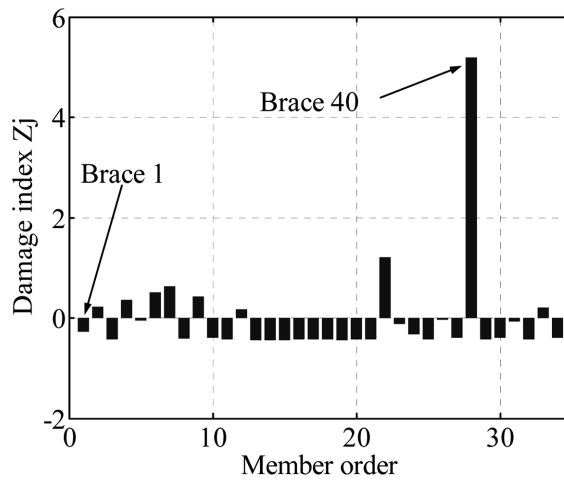


Fig. 12 Damage indices for Case 5

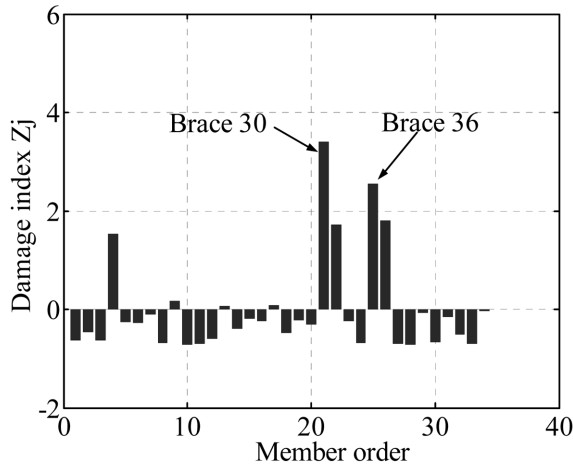


Fig. 13 Damage indices for Case 6

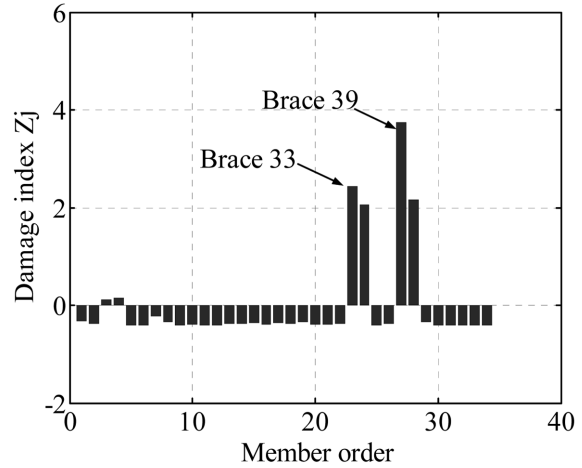


Fig. 14 Damage indices for Case 7

Fig. 12 shows the result of damage location for Case 5 that a slanted brace and a horizontal brace were damaged. It can be seen that the slanted brace is correctly located but the horizontal one is failed to be located. This also shows that horizontal brace is difficult to be located due to its structural redundancy when using all the first three modes.

Figs. 13 and 14 show the results of damage location for Case 6 and Case 7 where a slanted brace is partly damaged. It can be observed that the damage location for the partly damaged brace is correctly predicted but one false prediction is found similarly in the two cases. And the false predicted brace is just on the same floor and the opposite plane of the partly damaged brace.

### 3.4 Evaluation of damage severities

For evaluation of damage severities, only the cases with member severance are introduced since the evaluation for cases with partly damaged member is not available by experiments. Theoretic analysis on damage severities is also carried out using FEM models. Corresponding to the first five damage cases in Table 2, five FEM models damaged are created. Using the natural frequencies and

Table 4 Evaluated damage severities from FEM analysis and experiment

Case	Damaged member	Evaluated damage severity (%)		
		FEM analysis (Three-dimensionalmode shapes)	FEM analysis (Two-dimensionalmode shapes)	Experiment resultt
1	Slanted brace 30	70.8	33.8	56.7
2	Slanted brace 39	75.3	44.8	46.4
3	Slanted brace 40	72.2	48.1	57.2
	Slanted brace 30	58.8	24.8	24.1
4	Horizontal brace 1	0.12	----	----
5	Slanted brace 40	88.8	75.0	52.2
	Horizontal brace 1	----	----	----

Damage severity: the reduction percentage in Young's modulus.

12-point mode shapes of the first three modes from the undamaged and damaged FEM models, the damage severities are evaluated using three-dimensional and two-dimensional ( $Z$  values are set to be zero) modal shapes respectively. Table 4 shows the two results denoted as FEM analysis as well as the evaluation results of damage severities using the identified modal parameters from the undamaged and damaged experiment models. Matrices from the FEM model without model updating are also used for the calculations.

Firstly, from the results of FEM analysis, it can be seen that the evaluated damage severities using three-dimensional modal shapes are all smaller than the real values of 100%. It is evident that there exists a systematic error causing the damage severity to be underestimated slightly. As a matter of fact, from Eq. (10), it is noted that in order to have damage of 100%,  $\beta_j$  should have an infinite value. However Eqs. (7) and (9) show that  $\beta_j$  is always a finite number as  $Den$  is never null. So, in any case, it is impossible to estimate a damage of 100% thus leading to the underestimation. Also it can be noted that the evaluated damage severities using two-dimensional modal shapes are all smaller than those using three-dimensional modal shapes from FEM analysis. It is demonstrated the  $Z$ -value changes of modal shapes also have some weight for evaluation of damage severities. Secondly, from the results of experiment using two-dimensional identified modal shapes, it can be seen that the evaluated damage severities for slanted braces in five cases are all good enough in contrast with the results from the FEM analysis. And the damage severities for horizontal braces in Case 4 and 5 cannot be evaluated by experiment as well as by FEM analysis due to their structural redundancy.

#### 4. Conclusions

A model experiment to verify the damage detection algorithm based on partial measurement of vibration, which was designed to adapt to the circumstances of offshore jacket platforms, was presented in this paper. Damage location and severity evaluation were carried out for an experiment platform model under white-noise ground excitation using modal parameters from the ARMA identification. Modal parameters from FEM analysis were also employed to help the discussions. The main conclusions from the present study can be summarized as follows:

- (1) The damage detection algorithm is feasible on damage location and severity evaluation for broken slanted braces, but it is impractical for broken horizontal braces due to their structural redundancy. The damage detection algorithm is feasible on damage location for partly damaged slanted braces but may make false prediction for undamaged brace.
- (2) The damage detection algorithm is robust against the errors of baseline FEM model to real structure when the principal errors is formed by difference of modal frequencies not by mode shapes, so model updating is not needed for it.
- (3) The  $Z$ -value changes of modal shapes play a role in the precise detection of damage. Error prediction on damage location and underestimation of damage severity may occur when  $Z$  values of modal shapes are ignored in calculation.

#### Acknowledgements

The authors are grateful to Tetsuya Matsui, Professor of the Department of Architecture in Meijo University of Japan, for his early theoretic supervise on the project.

## References

- Brincker, R., Kirkegaard, P.H., Andersen, P. and Martinez, M.E. (1995), "Damage detection in an offshore structure", *Proc. of the 13th Int. Modal Analysis Conf.*, Nashville, Tennessee, 661-667.
- Della Greca, A. (1997), "Offshore facility management: how to render rational the underwater inspection and removal planning", *Proc. of the 16th Int. Conf. on Offshore Mechanics and Arctic Engineering*, Yokohama, Japan, ASME, **II**, 251-259.
- Doebling, S.W., Farrar, C.R. and Prime, M.B. (1998), "A summary review of vibration-based damage identification methods", *Shock Vib. Digest*, **205**(5), 631-645.
- Fukunaga, K. (1990), *Introduction to Statistical Pattern Recognition*, Academic Press, New York.
- Kanazawa, K. and Hirata, K. (2000), "Modal identification for a multi degree of freedom system using cross spectrum method", *J. Struct. Constr. Eng.*, Architectural Inst. Japan, (529), 89-96 (in Japanese).
- Kim, J.T. and Stubbs, N. (1995), "Damage detection in offshore jacket structures from limited modal information", *Int. J. Offshore Polar Eng.*, **5**(1), 58-66.
- Kim, J.T. and Stubbs, N. (2002), "Improved damage identification method based on modal information", *J. Sound Vib.*, **252**(2), 223-238.
- Kondo, I. and Hamamoto, T. (1994), "Local damage detection of flexible offshore platforms using ambient vibration measurement", *Proc. of the 4th Int. Symposium on Offshore and Polar Engineering*, Osaka, Japan, **IV**, 400-407.
- Mangal, L., Idichandy, V.G. and Ganapathy, C. (2001), "Structural monitoring of offshore platforms using impulse and relaxation response", *Ocean Eng.*, **28**(6), 689-705.
- Nichols, J.M. (2003), "Structural health monitoring of offshore structures using ambient excitation", *Appl. Ocean Res.*, **25**(3), 101-114.
- Roesset, J.M. and Yao, J.T.P. (1998), "Applications of structural health monitoring and damage detection to marine systems", *Proc. of the Second World Conf. on Structural Control*, Kyoto, Japan, **3**, 2327-2334.
- Ruotolo, R., Surace, C. and Worden, K. (2000), "Application of two damage detection techniques to an offshore platform", *Shock Vib. Digest*, **32**(1), 30-31.
- Sanderson, D.J., Price, A.G., Nelson, A., Thurlbeck, S.D., Killbourn, S. and Dougan, A. (2002), "The applicability of online monitoring for the assurance of fixed jacket structures' structural integrity", *Proc. of the Int. Conf. on Offshore Mechanics and Arctic Engineering*, OMAE, Oslo, Norway, **3**, 589-598.
- Shi, X., Matsui, T., Mizuno, K. and Ohmori, H. (2005), "Damage detection in offshore jacket platforms based on partial measurement", *J. Struct. Constr. Eng.*, Architectural Inst. Japan, (591), 169-177.
- Stacey, A. and Sharp, J.V. (1997), "Fatigue damage in offshore structures – causes, detection and repair", *BOSS'97 Behaviour of Offshore Structures*, Delft, The Netherlands, July, **3**, 77-91.
- Yang, H.Z., Li, H.J. and Wang, S.Q. (2003), "Damage localization of offshore platform under ambient excitation", *China Ocean Eng.*, **17**(4), 495-504.